Optimal Node Density for Detection in Energy Constrained Random Networks

Animashree Anandkumar, *Student Member, IEEE,*, Lang Tong[†], *Fellow, IEEE* and Ananthram Swami, *Fellow, IEEE*

Abstract—The problem of optimal node density maximizing the Neyman-Pearson detection error exponent subject to a constraint on average (per node) energy consumption is analyzed. The spatial correlation among the sensor measurements is incorporated through a Gauss-Markov random field model with Euclidean nearest-neighbor dependency graph. A constant density deployment of sensors under the uniform or Poisson distribution is assumed. It is shown that the optimal node density crucially depends on the ratio between the measurement variances under the two hypotheses and displays a threshold behavior. Below the threshold value of the variance ratio, the optimal node density tends to infinity under any feasible average energy constraint. On the other hand, when the variance ratio is above the threshold, the optimal node density is the minimum value at which it is feasible to process and deliver the likelihood ratio (sufficient statistic) of the sensor measurements to the fusion center. In this regime of the variance ratio, an upper bound on the optimal node density based on a proposed 2-approximation fusion scheme and a lower bound based on the minimum spanning tree are established. Under an alternative formulation where the energy consumption per unit area is constrained, the optimal node density is shown to be strictly finite for all values of the variance ratio and bounds on this optimal node density are provided.

Index Terms—Distributed detection, Gauss-Markov random fields, routing, error exponent, and sensor networks.

I. Introduction

WE consider the problem of distributed detection with a network of sensors that take measurements from one of the two unknown simple hypotheses, $\mathcal{H}_0$ and $\mathcal{H}_1$. Under the alternative hypothesis $\mathcal{H}_1$, sensors observe a Gauss-Markov random field (GMRF), and hence, have statistically correlated samples, which in practice indicates the presence of a phenomenon of interest. Under the null hypothesis $\mathcal{H}_0$, on the other hand, the sensors observe statistically independent measurements. Sensors deliver their measurement data to a fusion center where a test is made to determine the underlying hypothesis. We impose a constraint on the energy consumption

(a) n nodes in area $\frac{n}{\lambda}$ Asymptotic: $n \to \infty$ Constant density λ

(b) $\mathcal{H}_1$: GMRF, nearest-neighbor dependency graph
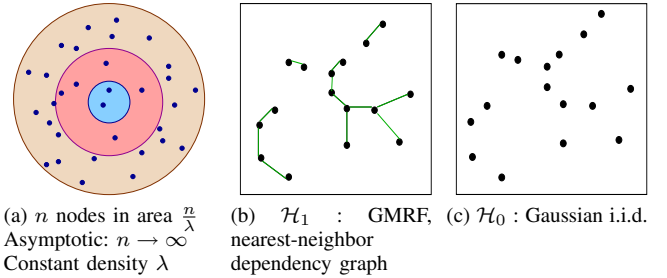
(c) $\mathcal{H}_0$: Gaussian i.i.d.

Fig. 1. Detection problem and random node deployment.

of the fusion process, consisting of multi-hop routing with in-network processing. Such a fusion process can result in considerable energy savings and is in contrast to classical routing, where no processing occurs at any intermediate nodes between the source and the destination.

Classical distributed detection often makes the so-called conditional i.i.d. assumption in which observations at different sensors are statistically independent and identically distributed conditioned on each hypothesis. Such an assumption effectively decouples detection performance from energy constraints: the number of sensor measurements used for data fusion (along with optimal sensor quantization and fusion rules) determines the detection performance whereas the energy consumed in data fusion is determined by the locations of the sensors involved. Typically, one prefers to collect data from sensors near the fusion center, which implies that sensors should be densely deployed.

On the other hand, when sensor measurements are correlated, the locations of the sensors affect not only the energy consumption but also the correlation structure of the measurements. Densely deployed sensors tend to have highly correlated measurements, which may either be beneficial or detrimental to detection efficiency.

In this paper, we consider the optimization of sensor density of a multi-hop sensor network in the context of energy-constrained distributed detection. For large sensor networks, it is unrealistic to optimize individual sensor locations. It is then natural to consider random deployment of sensors where the sensor density becomes the key design parameter. Optimizing sensor density is not only important for sensor deployment but also gives a simple decentralized sensor transmission strategy by deciding to transmit under independent coin flips.

To characterize the detection performance, we consider the Neyman-Pearson (NP) error exponent D. Our objective is to
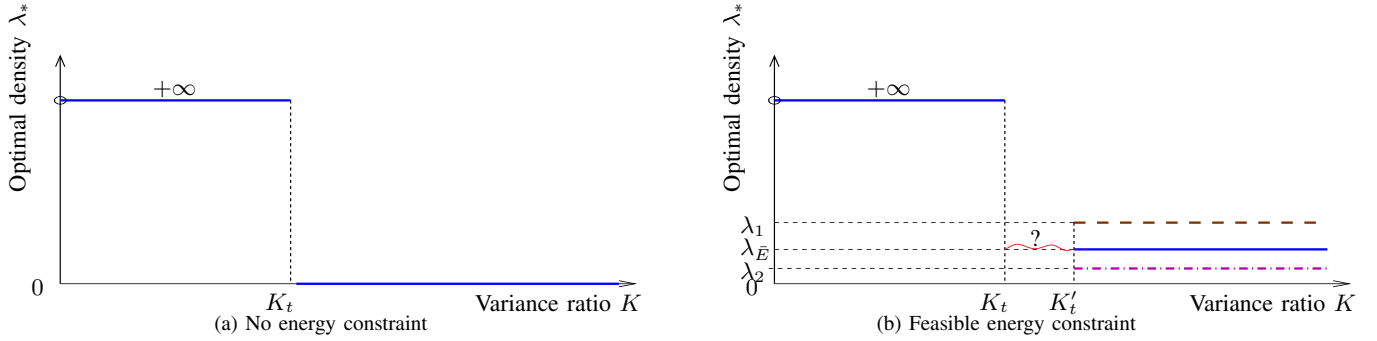
Fig. 2. Optimal node density vs. ratio of variances under $\mathcal{H}_1$ and $\mathcal{H}_0$. See Theorem 4. For a given energy constraint, $\lambda_2 \leq \lambda_* = \lambda_{\bar{E}} \leq \lambda_1$, for $K > K'_t$.

find an optimal node density λ_* that maximizes the detection error exponent D_λ, under a constraint $\bar{E}$ on the average (per node) energy consumption $\bar{C}(\lambda)$, when the number of nodes goes to infinity.

$$\lambda_* := \arg\max_{\lambda > 0} D_\lambda \quad \text{subject to } \bar{C}(\lambda) \leq \bar{E}. \tag{1}$$

We address the following questions: does an optimal node density exist? And if so, what is its value? Is it one of the extremes, viz., zero or infinity? This is an important question, since if the optimal node density is either zero or infinity, then we can simply place the nodes in as small or large an observation area as possible.

II. RELATED WORK

In many realistic scenarios sensor measurements are correlated, and our framework takes this into account. In general, spatial signals are acausal in contrast to temporal signals. In the literature, the two are usually distinguished by referring to acausal signals as random fields and to causal signals as random processes. Various assumptions on spatial correlation have been made in the literature. Joint-Gaussian distributions and distance-based correlation function have been widely assumed due to their simplicity [4]–[7]. Alternatively, diffusion-based models [8] and joint-entropy based models [9] have also been employed. All these models can be incorporated under the Markov random fields (MRF) framework. Markov random fields, also known as conditional auto-regressions, were introduced by Besag [10], [11]. The use of the MRF model for spatial data in sensor networks is relatively new (e.g., [12]), although it is widely used in image processing [13] and geo-statistics [14].

Detection of a Gauss-Markov random field (GMRF) is related to the detection of a Gauss-Markov random process (GMRP), which is a classical problem [15]. There is an extensive literature on the large-deviations approach to the analysis of detection of GMRP, e.g., [16], [17]. However, GMRP is not easily applicable to random placement of nodes in planar and higher dimensional spaces. Hence, we employ the model of a GMRF for randomly placed sensors on the Euclidean plane.

We are interested in routing spatially-correlated data for optimal detection and hence, there can be data fusion enroute to the fusion center. Such in-network processing algorithms

for computing certain aggregate functions are dealt in the surveys [18], [19]. These data-aggregation schemes, however, are applicable for optimal detection, only for conditionally independent data. An overview of routing in wireless networks can be found in [20].

The literature considering the tradeoff between detection performance and routing energy consumption is less extensive. In [21]–[23], energy-efficient detection is considered under various formulations. However, they all assume that the measurements are conditionally independent. Detection of one-dimensional GMRP is considered in [24], [25]. A specific link cost for detection, based on the Chernoff information, is proposed in [24]. In [25], a energy-density constraint is imposed, i.e., energy per unit distance is fixed, and a finite sensor density is shown to be optimal. But these works assume a one-dimensional model, not applicable when the nodes are on a plane. In [26], non-parametric target detection is studied; binary decisions are fused locally by a majority rule before transmission to a fusion center. However, no guarantee is provided on the energy savings obtained. In [27], a decision-theoretic approach to local inference of a Markov random field with single-bit communication is considered and the network topology is predefined by a directed acyclic graph.

In [28]–[30], we consider minimum-energy fusion and energy-detection tradeoff for general Markov-random field dependencies and arbitrary node placements. We show a Steiner tree construction for the optimal scheme and a preliminary version of this work focusing on nearest-neighbor dependency appears in [3]. In contrast, an alternative formulation is considered in this paper with random point sets, which enables us to explicitly characterize scaling laws, as the number of nodes goes to infinity, for both the detection performance and the average energy consumption for data fusion, and derive optimal node density using these results. An abbreviated version of some results of this paper appears in [1]. In this paper, we provide additional results on lower and upper bounds for the optimal density under per-node energy constraint. We also consider an alternative formulation where the energy consumption per unit area is instead constrained.

III. OVERVIEW OF RESULTS AND APPROACH

Given a per-node energy budget for data fusion, we aim to find the sensor density that optimizes the detection performance. Assuming that all the nodes have the same measure-

ment variance σ_j^2 under each hypothesis $\mathcal{H}_j$, we define the variance ratio as

$$K := \frac{\sigma_1^2}{\sigma_0^2}. \qquad (2)$$

The main results demonstrate the presence of a threshold K_t effect on the variance ratio K. As shown in Figure 2, when K is below a threshold K_t, the optimal density is unbounded, and thus it is optimal to concentrate sensors near the fusion center. Moreover, this result is independent of the energy constraint implying that imposing an energy constraint does not degrade detection performance. On the other hand, when K is above the threshold K_t and no energy constraint is imposed, the optimal density tends to zero (Fig. 2a), which in practice, implies that it is optimal to disperse sensors in the largest possible area. In this regime of K, imposing an energy constraint leads to a strictly finite optimal density and we provide bounds on this optimal value (Fig. 2b).

We give a closed-form expression for the threshold K_t on the variance ratio K which decides the behavior of the optimal density. The threshold K_t is independent of the energy constraint. Moreover, somewhat surprisingly, it depends on the correlation structure only through the limiting correlation of two sensors as their separation distance vanishes.

We also investigate the use of an energy density constraint where the total energy consumption in a given area is constrained instead of the average energy at each node. We show that an optimal node density under this formulation exists, and is strictly finite for all values of the variance ratio K. This is in sharp contrast to the threshold behavior under a per-node energy constraint. We prove analytical bounds for the optimal density when the variance ratio $K < 2$.

A brief comment on the approach adopted is in order. Our approach relies on the characterization of detection error exponent and energy consumption for data fusion when the sensors are randomly deployed with constant density. Note that in general, both the error exponent and the energy consumption are indeed governed by the entire correlation structure. But we prove that for a Markov random field model these quantities are only dependent on the "local" correlation behavior. The key technique is the law of large numbers (LLN) for functionals on random graphs, recently obtained by Yukich and Penrose [31]. In essence, the LLN states that the limit of a global functional on a random graph tends to a "local" effect around the origin under some conditions. Using the LLN, we have derived a closed-form expression for the detection error exponent in [2].

In this paper, we use the LLN to derive scaling laws for energy consumption involved in data fusion for detection. Finding the optimal fusion scheme with minimum energy consumption is intractable. We have shown that this is equivalent to a Steiner tree, and hence is NP-hard for any arbitrary node placement [28], [29]. Here, we analyze DFMRF, a 2-approximate fusion scheme, i.e., with energy consumption no more than twice that of the optimal scheme. This analysis is significant on its own because the DFMRF fusion scheme is implementable in practice and results in significant savings in energy consumption. In this paper, we strengthen the approximation guarantee of the DFMRF scheme for random node placement from 2 to a constant that depends on the channel path-loss exponent using the LLN. In the process, we also prove that the DFMRF fusion scheme has a constant asymptotic average energy consumption, in contrast to the classical approach of sending all the raw data to the fusion center on shortest paths, which has an almost linear scaling, as depicted in Fig.5. Finally, we employ this scaling result as a vehicle to provide bounds on the optimal node density when the variance ratio K is above threshold K_t, as seen in Fig.2b.

Our paper is organized as follows. The system model is explained in section IV. The detection problem is specified in section V and minimum energy routing in section VI. Asymptotic analysis of routing energy and detection performance is provided in section VII. Results on optimal density are in section VIII and numerical analysis in section VIII-D. The energy-density formulation is dealt in section IX. Section X concludes the paper.

IV. SYSTEM MODEL

An undirected graph $\mathcal{G}$ is a tuple $\mathcal{G} = (\mathcal{V}, \mathcal{E})$ where $\mathcal{V}$ is the vertex set and $\mathcal{E} = \{(i,j), \ i,j \in \mathcal{V}, i < j\}$ is the edge set. Let R_{ij} be the random variable denoting the Euclidean edge-length of (i,j). The neighborhood function of a node i is the set of all other nodes having an edge with it. For a directed graph, we denote the edges by $\mathcal{E} = \{<i,j>, i,j \in \mathcal{V}, i \neq j\}$, where the direction of the edge is from i to j.

For the matrix $\mathbf{A} = [A(i,j)]$, $A(i,j)$ denotes the element in the ith row and j^{th} column and $|\mathbf{A}|$ its determinant. For two sets A and B, let $A \backslash B = \{i : i \in A, i \notin B\}$.

A. Gauss-Markov Random Field

A GMRF, in addition to being a Gaussian random field, satisfies special conditional independence properties. A simple example is the first-order auto-regressive process, where the conditional independence of the observations is based on causality. However, a spatial random field has a far richer set of conditional independencies, requiring a more general definition [32, p. 21].

Definition 1 (GMRF): Given a point set $\mathcal{V} = \{1, \ldots, n\}$, $\mathbf{Y}_{\mathcal{V}} = \{Y_i : i \in \mathcal{V}\}$ is a GMRF with an (undirected) dependency graph $\mathcal{G}_d(\mathcal{V}, \mathcal{E}_d)$ if $\mathbf{Y}_{\mathcal{V}}$ is a Gaussian random field, and $\forall i,j \in \mathcal{V}$, Y_i and Y_j are conditionally independent given observations at all other nodes if i and j are not neighbors,

$$Y_i \perp Y_j | \mathbf{Y}_{-ij} \iff (i,j) \notin \mathcal{E}_d, \ \forall i,j \in \mathcal{V}, i \neq j, \quad (3)$$

where $\perp$ denotes conditional independence and $\mathbf{Y}_{-ij} := (Y_k : k \in \mathcal{V}, k \neq i,j)$.

B. Network and Energy Model

We assume that the energy consumed by a node i can be represented by the sum of a constant processing energy $C_p > 0$ and the transmission energy[1] [33]. For details, see [3]. The

---

[1] We ignore the energy consumed at the receiver.

energy required for the transmission of a real number from i to j is denoted by $C_{i,j}$. We assume that

$$C_{i,j} = C_t |\text{dist}(i,j)|^\nu, \, 2 \le \nu \le 4, \quad (4)$$

where C_t is a constant, $\text{dist}(i,j)$ is the inter-node distance and ν is the channel path-loss exponent. Further, we assume that the processing energy C_p at every node is constant and independent of the number of transmissions from the node, and hence, can be ignored in the optimization framework.

The set of transmissions within a node set $\mathcal{V}$ can be represented as a digraph $\mathcal{G}_t = (\mathcal{V}, \mathcal{E}_t)$. Note that this transmission digraph $\mathcal{G}_t$ is different from the dependency graph $\mathcal{G}_d$ of the signal field. Let $\mathbf{C}(\mathcal{G}_t)$ denote the total transmission energy given by

$$\mathbf{C}(\mathcal{G}_t) := C_t \sum_{e \in \mathcal{E}_t} R_e^\nu, \quad (5)$$

where R_e is the Euclidean edge length. We require that $\mathcal{G}_t \subset \text{UDG}(\mathcal{V})$, the unit-disk graph, defined as the set of edges between any two nodes within an unit Euclidean distance of each other. We further require $\mathcal{G}_t$ to deliver the log-likelihood ratio (LLR) to the fusion center to ensure optimal detection, which is explained in detail in the next section.

V. HYPOTHESIS-TESTING PROBLEM

Let $\mathcal{V} = \{1, \ldots, n\}$ be a set of n nodes on the plane and let $\mathbf{Y}_n$ be the random vector of observation samples $Y_i, i \in \mathcal{V}$,

$$\mathbf{Y}_n := [Y_1, \ldots, Y_n]^T. \quad (6)$$

The hypothesis-testing problem is

$$\mathcal{H}_0 : \mathbf{Y}_n \sim \mathcal{N}(\mathbf{0}, \sigma_0^2 \mathbf{I}) \quad \text{vs.} \quad \mathcal{H}_1 : \mathbf{Y}_n \sim \mathcal{N}(\mathbf{0}, \mathbf{\Sigma}_{1,\mathcal{V}}), \quad (7)$$

where the covariance matrix $\mathbf{\Sigma}_{1,\mathcal{V}}$ of a GMRF depends on the configuration of nodes in $\mathcal{V}$. See Fig.1b and Fig.1c.

The optimal decision-rule under the Neyman-Pearson formulation is a threshold test based on the log-likelihood ratio (LLR). Let $p[\mathbf{Y}_n | \mathcal{V}; \mathcal{H}_j]$ be the conditional PDF of the observations given the point set $\mathcal{V}$ under hypothesis j, for $j = 0, 1$. Then, the LLR is given by

$$\text{LLR}(\mathbf{Y}_n, \mathcal{G}_d) := \log \frac{p[\mathbf{Y}_n, \mathcal{V}; \mathcal{H}_0]}{p[\mathbf{Y}_n, \mathcal{V}; \mathcal{H}_1]}. \quad (8)$$

In order to conduct optimal detection at the fusion center, it suffices to deliver the LLR to the fusion center and raw data is not needed. Such data fusion schemes are outlined in Section VI.

A. Covariance matrix of GMRF

We make an additional assumption on the structure of the covariance matrix $\mathbf{\Sigma}_{1,\mathcal{V}}$ of the GMRF under $\mathcal{H}_1$ viz., that the nodes have the same measurement variance for any node configuration $\mathcal{V}$, i.e.,

$$\mathbf{\Sigma}_{1,\mathcal{V}}(i,i) := \sigma_1^2, \; i = 1, \ldots, n. \quad (9)$$

We denote the ratio between the variances under the alternative and the null hypothesis at each node by

$$K := \frac{\sigma_1^2}{\sigma_0^2}.$$

We also assume that under $\mathcal{H}_1$, the amount of correlation between the neighbors i, j of the dependency graph is specified by an arbitrary function g, which has the Euclidean edge length R_{ij} as its argument. From (9), we have

$$g(R_{ij}) := \frac{\mathbf{\Sigma}_{1,\mathcal{V}}(i,j)}{\sigma_1^2}, \; \forall \, (i,j) \in \mathcal{E}. \quad (10)$$

The correlation function g is required to satisfy some regularity conditions. We assume that

$$g(0) := M < 1, \quad g(\infty) = 0, \quad (11)$$

and that g is a monotonically decreasing convex function of the edge length. This is a reasonable assumption, since the amount of correlation usually decays as nodes become farther apart. Moreover, partial correlation or $g(0) = M < 1$ arises due to signal imperfections. Note that this has the same effect on correlation as imposing an exclusion region on how near two nodes can be placed. Some examples of the correlation functions, satisfying our assumptions, are

$$g(R) = M e^{-aR}, \; g(R) = \frac{M}{1 + R^a}, \; 0 \le a, M < 1.$$

Note that we do not assume the presence of additive Gaussian measurement noise in the signal model, as considered in the literature before. This is because with the additive noise, the resulting GMRF no longer has a sparse dependency graph. As an alternative formulation, we model imperfect measurements by assuming partially-correlated nodes.

B. Nearest-neighbor graph

Typically, spatial interactions are based on proximity, where the choice of edges is determined by the local point configuration according to some specified rule [34]. With a regular lattice structure (e.g., in image processing, Ising model), a fixed set of neighbors can be specified in a straight-forward manner [35]. However, the situation is more complicated for arbitrarily placed nodes. In this paper, we assume the dependency graph $\mathcal{G}_d$ to be the nearest-neighbor graph (NNG), which is the simplest proximity graph. The nearest-neighbor function of a node $i \in \mathcal{V}$, is defined as,

$$\text{nn}(i) := \arg \min_{j \in \mathcal{V}, j \ne i} \text{dist}(i,j), \quad (12)$$

4

where dist$(\cdot, \cdot)$ is the Euclidean distance. The nearest-neighbor (undirected) graph $\mathcal{G}_d(\mathcal{V}, \mathcal{E}_d)$ is formally given by

$$(i, j) \in \mathcal{E}_d \iff i = \text{nn}(j) \text{ or } j = \text{nn}(i). \quad (13)$$

C. Expression for log-likelihood ratio

We incorporate the assumptions (9-10) on the covariance matrix in the theorem below to obtain the LLR in (8) for detection.

Theorem 1 (Log-likelihood ratio): Under the assumptions (9-10), the log-likelihood ratio in (8) for the hypothesis-testing problem in (7), given point set $\mathcal{V} = \{1, \ldots, n\}$, is

$$
\begin{aligned}
\text{LLR}(\mathbf{Y}_n, \mathcal{G}_d) &= n \log \frac{\sigma_1}{\sigma_0} + \frac{1}{2} \left[\sum_{i \in \mathcal{V}} \left(\frac{1}{\sigma_1^2} - \frac{1}{\sigma_0^2} \right) Y_i^2 \right. \\
&+ \sum_{(i,j) \in \mathcal{E}} \left\{ \log[1 - g^2(R_{ij})] \right. \\
&+ \frac{g^2(R_{ij})}{1 - g^2(R_{ij})} \frac{Y_i^2 + Y_j^2}{\sigma_1^2} \\
&\left. \left. - \frac{2g(R_{ij})}{1 - g^2(R_{ij})} \frac{Y_i Y_j}{\sigma_1^2} \right\} \right],
\end{aligned}
\quad (14)
$$

where R_{ij} is the Euclidean edge length of $(i, j) \in \mathcal{E}$.

Theorem 1 gives a closed-form expression for the log-likelihood ratio, in terms of the edges of the nearest-neighbor dependency graph of the GMRF. Note in (14), the cross-terms are only between the neighbors of the dependency graph, which is exploited to yield explicit data-fusion scheme (DFRMF) [3], summarized in section VI. Note that (14) contains two kinds of terms. The *edge potentials*, denoted by $\phi_{i,j}(Y_i, Y_j)$, that depend on a pair of observations, are given by
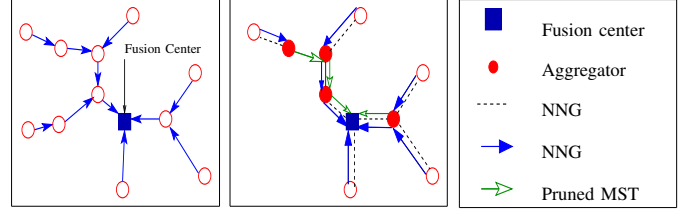
$$
\begin{aligned}
\phi_{i,j}(Y_i, Y_j) &:= \frac{1}{2} \log[1 - g^2(R_{ij})] - \frac{g(R_{ij})}{1 - g^2(R_{ij})} \frac{Y_i Y_j}{\sigma_1^2} \\
&+ \frac{g^2(R_{ij})}{1 - g^2(R_{ij})} \frac{Y_i^2 + Y_j^2}{2\sigma_1^2},
\end{aligned}
\quad (15)
$$

and the *node potentials* $\phi_i(Y_i)$, depending on a single observation, are given by

$$\phi_i(Y_i) := \log \frac{\sigma_1}{\sigma_0} + \frac{1}{2} \left(\frac{1}{\sigma_1^2} - \frac{1}{\sigma_0^2} \right) Y_i^2. \quad (16)$$

Hence, the LLR can be written in a compact form

$$\text{LLR}(\mathbf{Y}_n; \mathcal{G}_d) = \sum_{i \in \mathcal{V}} \phi_i(Y_i) + \sum_{(i,j) \in \mathcal{E}_d} \phi_{i,j}(Y_i, Y_j). \quad (17)$$

(a) MST is optimal for i.i.d. data.   (b) DFMRF routing for detection of MRF.   (c) Legend

Fig. 3.   Routing schemes for detection under different correlation models.

VI. MINIMUM ENERGY ROUTING

The aim of optimal minimum energy data fusion for detection is to ensure the delivery of the LLR, given by (17), to the designated fusion center while minimizing the total energy consumption. First consider the special case when the measurements are independent conditioned under either hypothesis. In this case, the LLR in (17) is just the sum of the node potentials and all the edge potentials are zero. The minimum-energy routing in this case is given by the directed minimum spanning tree (DMST), with the directions toward the fusion center. See Fig.3a. The sum function can be calculated hierarchically along the DMST, starting at the leaves and ending at the fusion center. This special case of independent measurements in fact, turns out to be a lower bound for energy consumption of any data fusion scheme.

Lemma 1 (Lower Bound for C_* [3]): The minimum energy consumption C_* for a data fusion scheme that delivers the LLR in (17) to the fusion center is at least the total energy consumption along the minimum spanning tree, i.e.,

$$C_* \geq C(\text{MST}). \quad (18)$$

The lower bound is achieved iff. the sensor data are independent, conditioned on either hypotheses.

Hence, the presence of correlation increases routing costs since the log-likelihood ratio in (17) is more complicated. In [28], we show that incorporating correlation makes minimum energy routing a NP-hard problem and hence, we have to focus on approximation algorithms. We employ a 2-approximation routing algorithm called the data fusion of a Markov random field (DFMRF), proposed in [3]. The approximation ratio ρ of a polynomial time algorithm implies that its value of the objective function is always no worse than ρ times the optimal value. We define the approximation ratio of the DFMRF as

$$\rho := \frac{C(\text{DFMRF})}{C_*}. \quad (19)$$

We restate the approximation guarantee of DFMRF below.

Lemma 2 (Approx. Ratio for DFMRF [3]): DFMRF is a 2-approximation algorithm for any arbitrary node placement.

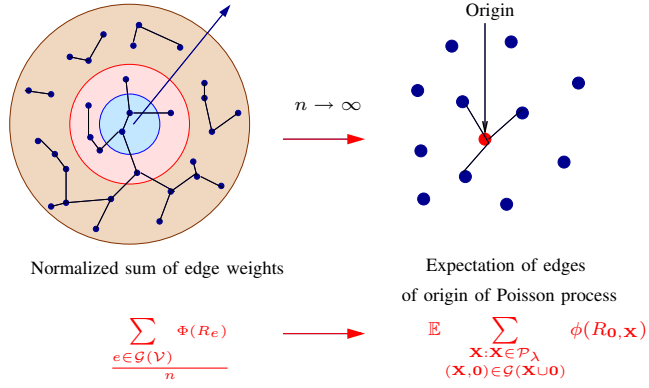$$\rho = \frac{C(\text{DFMRF})}{C_*} \leq 2. \quad (20)$$

Fig. 4. Pictorial representation of LLN for graph functionals of uniform or Poisson point sets.
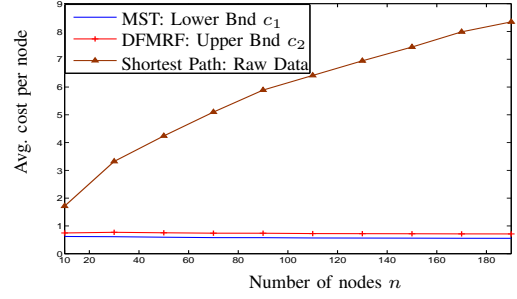

Fig. 5. Avg. per-node energy consumption for DFMRF scheme and shortest-path routing for nearest-neighbor dependency and uniform distribution. 500 simulation runs. Path-loss coefficient $\nu = 2$, $C_t, \lambda = 1$. See (4) and (24).

Hence, for any arbitrary node placement, the energy consumption of the DFMRF scheme is at most twice that of the optimal fusion scheme. Since we consider random point sets here, the approximation ratio can be improved by analyzing the asymptotic energy consumption and we undertake it in the next section.

The DFMRF scheme proceeds in two stages. In the first stage, sensor measurements are transmitted along the edges of the NNG. This ensures that the edge potentials in (17) are computed at various nodes (called the aggregators). In the next stage, the computed values are summed up along the edges of the pruned minimum spanning tree (MST), where pruning refers to the removal of leaves. Details about the DFMRF scheme can be found in [3]. A schematic of the DFMRF scheme is shown in Fig. 3b. From (4), the total energy consumption of the DFMRF scheme can be expressed as

$$\mathrm{C(DFMRF)} = C_t \left(\sum_{e \in \mathrm{NNG}} R_e^\nu + \sum_{e \in \mathrm{MST}} R_e^\nu - \sum_{e \in \mathcal{L}_f(\mathrm{MST})} R_e^\nu \right), \quad (21)$$

where $\mathcal{L}_f(\mathrm{MST})$ represents the leaves of the MST.

VII. ASYMPTOTIC ANALYSIS

It is intractable to analytically evaluate energy consumption or detection performance for an arbitrary node set. Therefore, we assume that the nodes are placed randomly, according to a point process defined on expanding regions, formally defined below. The number of nodes n goes to infinity, with fixed node density λ (Fig.1a).

Definition 2 (Poisson and Binomial Processes [36]): Let $(\mathcal{B}_n)_{n \geq 1}$ denote a sequence of squares or circles of area $\frac{n}{\lambda}$, centered at the origin, for any $\lambda > 0$. A binomial point process on $\mathcal{B}_n$, denoted by $\mathcal{U}_{n,\lambda}$, consists of n points distributed i.i.d. uniformly on $\mathcal{B}_n$. A homogeneous Poisson process of intensity λ on $\mathcal{B}_n$, denoted by $\mathcal{P}_{n,\lambda}$, satisfies the following properties:

1) for any set $\mathcal{A} \subset \mathcal{B}_n$ with area A, the number of points in $\mathcal{A}$ is Poisson distributed with mean λA,
2) for any $n \in \mathbb{N}$ and $\mathcal{A} \subset \mathcal{B}_n$ with area $A > 0$, conditioned on n number of points in $\mathcal{A}$, the point process on $\mathcal{A}$ is a binomial process.

Such a random node placement allows us to employ the law of large numbers (LLN) for graph functionals, briefly described below.

A. LLN for Graph Functionals

The law of large numbers (LLN) for functionals on graphs enables us to evaluate the error exponent and applies to graphs which are random in the sense that the vertex set is a marked random point set. LLN on graphs is based on the so-called *objective method*. Steele [37] coined this term for a philosophy whereby, loosely speaking, one describes the limiting behavior of functionals on finite point sets of binomial process in terms of related functionals defined on infinite Poisson point sets. Penrose and Yukich [31], [34], [38] introduced a concept of *stabilizing* functionals and use the objective method to establish a strong law of large numbers for graph functionals [31, P. 287]. The result is illustrated in Fig.4, where the limit of empirical average of the edge functionals of a stabilizing graph is the expectation over the sum of only the edge functionals of the origin, with the points drawn from an infinite Poisson process. Hence, the LLN states that the limit is a localized effect around the origin. The LLN is valid for stabilizing graphs, where the local behavior of the graph in a bounded region is unaffected by points beyond a finite (but random) distance from that region. The nearest-neighbor graph (NNG) is one such stabilizing graph with translation and scale-invariance [34, Lemma 6.1] and we focus on NNG dependency in this paper.

B. Average Energy for DFMRF

We now analyze the average energy consumption for the DFMRF scheme. The average energy for DFMRF under the binomial or Poisson process can be quantified using the law of large numbers (LLN) for graph functionals [31].

Theorem 2 (Optimal Average Energy): The asymptotic average energy consumption for the DFMRF scheme and for fusion along the minimum spanning tree (MST) are given by

$$\lim_{n \to \infty} \frac{\mathrm{C(DFMRF(\lambda))}}{n} = C_t \lambda^{-\frac{\nu}{2}} c_1(\nu), \quad (22)$$

$$\lim_{n \to \infty} \frac{\mathrm{C(MST(\lambda))}}{n} = C_t \lambda^{-\frac{\nu}{2}} c_2(\nu), \quad (23)$$

6

where $c_1(\nu)$ and $c_2(\nu)$ are constants, independent of λ, and ν is the channel path-loss coefficient in (4). Hence, the optimal average energy consumption for data fusion $\bar{C}_*$ satisfies the bounds

$$\lim_{n\to\infty} \frac{C(\text{MST}(\lambda))}{n} \leq \bar{C}_*(\lambda) \leq \lim_{n\to\infty} \frac{C(\text{DFMRF}(\lambda))}{n}$$
$$C_t \lambda^{-\frac{\nu}{2}} c_2(\nu) \leq \bar{C}_*(\lambda) \leq C_t \lambda^{-\frac{\nu}{2}} c_1(\nu). \quad (24)$$

This implies that the approximation ratio of the DFMRF under random node placement is improved to $\frac{c_1(\nu)}{c_2(\nu)}$.

Proof: The limit in (23) is proven in [38]. To evaluate the limit in (22), we use the expression in (21). We note that the power-weighted edges of the NNG, MST and the leaves of MST are all stabilizing graph functionals [38]. Therefore, the LLN for graph functionals holds and we have (22). For approximation ratio, we have

$$\lim_{n\to\infty} \frac{C(\text{DFMRF})}{C_*} \leq \lim_{n\to\infty} \frac{C(\text{DFMRF})}{C(\text{MST})} = \frac{c_1(\nu)}{c_2(\nu)}.$$

□

The constants $c_1(\nu)$ and $c_2(\nu)$ are the same for both the binomial and the Poisson process, and are evaluated through simulations. For a 500 node network, we obtained $c_1(2) = 0.7134$, $c_1(3) = 0.6462$ and $c_1(4) = 0.6528$. Similarly, for the lower bound $c_2(\nu)$, which is based on the MST, analysis and simulation results are available in [39].

In Fig.5, we plot simulation results comparing the average energy consumption of the DFMRF scheme (c_1) and the lower bound (c_2), based on the average energy consumption for fusion along the MST. We also plot the energy consumption for the classical approach using shortest paths to route all the raw data and we see that it does not have a constant-factor scaling. In fact, as the number of nodes grows the average energy consumption for shortest-path routing grows almost linearly. Hence, collecting all the raw data from a large network with energy constrained nodes is not feasible and our fusion scheme DFMRF is applicable in such scenarios.

C. Detection Error Exponent

In this section, we characterize the detection error exponent for the hypothesis testing problem in (7). Under the Neyman-Pearson criterion, for a fixed Type-I error bound, the exponent of the Type-II error is independent of the type-I error bound [17], and is given by

$$D := \lim_{n\to\infty} \frac{1}{n} \log \frac{p[\mathbf{Y}_n; \mathcal{H}_0]}{p[\mathbf{Y}_n | \mathcal{V}; \mathcal{H}_1]}, \quad \text{under } \mathcal{H}_0. \quad (25)$$

In the theorem below, we restate the closed form for the error exponent, derived[2] in [2], in terms of the variables and functions defined below.

[2]The expression given in [2] is in a different form, but reduces to (31).

$$f_1(x) := \log[1 - x^2], f_2(x) := \frac{2x^2}{[1 - x^2]}, \quad (26)$$

$$f(x, K) := f_1(x) + \frac{1}{K} f_2(x) \quad (27)$$

$$h_i(x; g) := f_i(g(x)) - \frac{\pi}{2\omega} f_i(g(\sqrt{\frac{\pi}{\omega}} x)), \quad (28)$$

$$h(x, K; g) := h_1(x; g) + \frac{1}{K} h_2(x; g), \quad (29)$$

where $g(\cdot)$ is the correlation function. Let Z denote the Rayleigh random variable with variance $(2\pi)^{-1}$ and let ω be the area of the union of two unit-radii circles with centers unit distance apart, given by

$$\omega = \frac{4\pi}{3} + \frac{\sqrt{3}}{2} \approx 5.06. \quad (30)$$

Theorem 3 (Expression for D [2]): For a GMRF on NNG with correlation function g, with the nodes drawn from the binomial or the Poisson process with node density λ and region area $\frac{n}{\lambda}$, the error exponent D for Neyman-Pearson detection is

$$D(\lambda, K; g) = \frac{1}{2} \Big[\mathbb{E}_\lambda h(Z\lambda^{-0.5}, K; g) + \log K + \frac{1}{K} - 1 \Big], \quad (31)$$

where $\mathbb{E}_\lambda$ is the expectation over the random variable Z.

Proof: An intermediate expression for D derived in [2] is given by

$$D(\lambda, K; g) = \frac{1}{2} \Big[\lim_{n\to\infty} \frac{1}{n} \sum_{e\in\text{NNG}} f(g(R_e), K; g) + \log K + \frac{1}{K} - 1 \Big] \quad (32)$$

We then employ the special law of large numbers for graph functionals [31] to obtain (31). Details can be found in [2].

□

Note that in (31), the expectation term captures the correlation structure of the GMRF and the remaining terms represent the detection error exponent for two i.i.d. Gaussian processes with variance ratio K, i.e.,

$$D(\lambda, K; g) = \frac{1}{2} \mathbb{E}_\lambda h(Z\lambda^{-0.5}, K; g) + D_{IID}(K), \quad (33)$$

where $D_{IID}(K)$ the error exponent when the measurements are conditionally i.i.d., and is given by

$$D_{IID}(K) = \frac{1}{2} \Big[\log K + \frac{1}{K} - 1 \Big]. \quad (34)$$

Hence, the effect of correlation on the error exponent is quantified in a compact form. It can be easily verified that the expectation term is zero, when $g(0) = M = 0$ (no correlation). It is easy to see that $D_{IID}(K)$ is independent of the node

density λ. Hence, the issue of optimal node density for error exponent arises only in the presence of correlation. Moreover, intuitively, as we vary node density λ, the edge lengths in the resulting NNG scale by the factor $\lambda^{-0.5}$, on an average. Hence, we see that this factor $\lambda^{-0.5}$ appears in the expectation term in (33).

VIII. OPTIMAL NODE DENSITY

Recall that our objective is to find an optimal node density λ_* maximizing the detection error exponent under a constraint on the average energy consumption of data fusion.

$$\lambda_* := \arg \max_{\lambda > 0} D_\lambda \quad \text{subject to } \bar{C}(\lambda) \leq \bar{E}.$$

We have so far derived a closed-form expression for the error exponent D_λ (short form for $D(\lambda, K; g)$ in (31)) and bounds for optimal average energy consumption $\bar{C}_*(\lambda)$ in (24). In this section, we exploit these expressions to derive the optimal node density.

Before proceeding to the actual derivations, it is useful to consider a special case, viz., when both the hypotheses have the same measurement variance ($K = (\frac{\sigma_1}{\sigma_0})^2 = 1$) and there is no energy constraint ($\bar{E} \to \infty$). Since there is no correlation under $\mathcal{H}_0$, the two hypotheses can be distinguished only by the presence of correlation under $\mathcal{H}_1$. Correlation is maximized when all the nodes are clustered close to one another, since correlation decays with distance. Hence, the optimal density should be infinite. We prove that this is indeed true and also characterize the optimal density for general K and energy constraint $\bar{E}$. To this end, we first characterize the set of feasible node densities which can support data fusion under the given energy constraint $\bar{E}$.

A. Feasible Node Density Set

In order to incorporate the energy constraint $\bar{E}$, we need to find a feasible set Λ of node densities for minimum energy routing that satisfies the average energy constraint $\bar{E}$ and delivers the LLR to the fusion center,

$$\Lambda(\bar{E}) := \{\lambda : \bar{C}_*(\lambda) \leq \bar{E}\}. \tag{35}$$

When the density goes to infinity, the optimal average energy consumption for routing goes to zero

$$\lim_{\lambda \to \infty} \bar{C}_*(\lambda) = 0.$$

This is derived from the bounds on $\bar{C}_*$ in (24). Hence, the energy constraint $\bar{E}$ is satisfied at infinite density or in other words, $\lambda \to \infty \in \Lambda$ for Λ defined in (35). Hence, whenever Λ is non-empty, it is of the form

$$\Lambda(\bar{E}) = [\lambda_{\bar{E}}, \infty], \tag{36}$$

where $\lambda_{\bar{E}}$ is defined as the minimum node density under the energy constraint $\bar{E}$ at which it is feasible to perform data fusion. However, as discussed in Section VI, finding the minimum energy scheme is NP-hard. Hence, finding an expression

for $\lambda_{\bar{E}}$ is analytically intractable. We instead provide bounds on $\lambda_{\bar{E}}$ using (24).

We first consider feasible node density for DFMRF scheme. From (22), imposing the energy constraint $\bar{E}$ translates to a constraint on λ under the DFMRF,

$$\bar{C}(\text{DFMRF}(\lambda)) \leq \bar{E} \iff \lambda \geq \lambda_1(\bar{E}) := \left(\frac{\bar{E}}{C_t c_1(\nu)}\right)^{\frac{2}{\nu}}. \tag{37}$$

Similarly, from (23), imposing the constraint $\bar{E}$ for data fusion along the edges of the MST leads

$$\bar{C}(\text{MST}(\lambda)) \leq \bar{E} \iff \lambda \geq \lambda_2(\bar{E}) := \left(\frac{\bar{E}}{C_t c_2(\nu)}\right)^{\frac{2}{\nu}}. \tag{38}$$

From the bounds on optimal average energy in (24), we have bounds on the feasible set of node densities Λ for the minimum energy scheme,

$$\{\lambda : \lambda \geq \lambda_2(\bar{E})\} \subset \Lambda(\bar{E}) \subset \{\lambda : \lambda \geq \lambda_1(\bar{E})\}. \tag{39}$$

From the definition of $\lambda_{\bar{E}}$ in (36), we have

$$\lambda_2(\bar{E}) \leq \lambda_{\bar{E}} \leq \lambda_1(\bar{E}). \tag{40}$$

Hence, although we are unable to evaluate $\lambda_{\bar{E}}$, we have bounds that are easily evaluated.

B. Infinite Node Density

We first analyze the error exponent D, when the node density λ goes to infinity. This will provide insights for finding the optimal density. As $\lambda \to \infty$, we have

$$D(\infty, K; g) = D_{IID}(K) + \frac{1}{2} h(0, K, M),$$

where $h(0, K; g)$ depends on g only through $g(0) = M$, and

$$h(0, K, M) = (1 - \frac{\pi}{2\omega})\left(\log[1 - M^2] + \frac{2M^2}{K[1 - M^2]}\right). \tag{41}$$

In the theorem below, we prove that the presence of correlation can either improve or degrade the error exponent, depending on the variance ratio K. We establish a threshold on K that determines the transition.
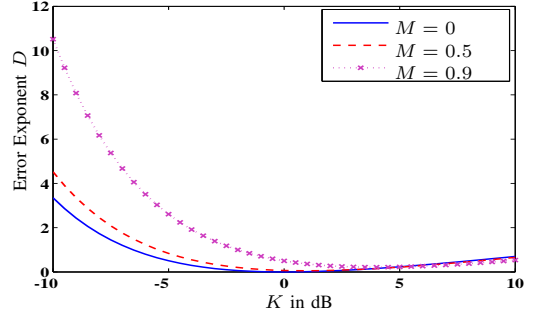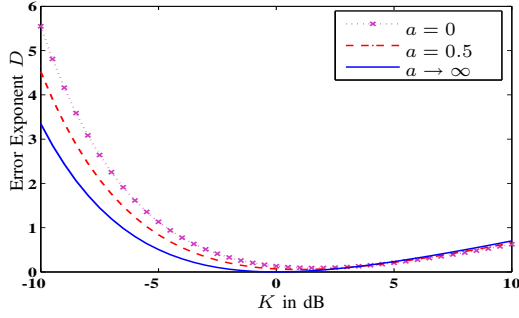
Lemma 3 (Behavior at Infinite Density ($\lambda \to \infty$)): At $\lambda \to \infty$, the correlation term $h(0, K, M)$ in (41) is positive, if the variance ratio K is below a threshold value $K_t(M)$,

$$h(0, K, M) \begin{cases} \geq 0, & \text{for } K < K_t(M), \quad \text{(42a)} \\ < 0, & \text{for } K > K_t(M). \quad \text{(42b)} \end{cases}$$
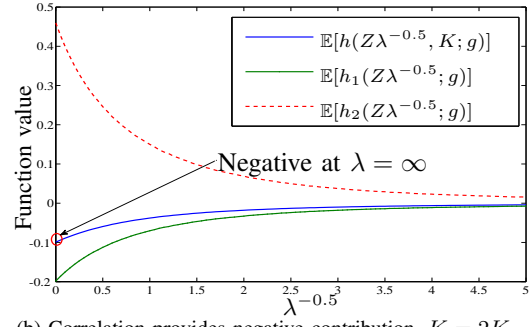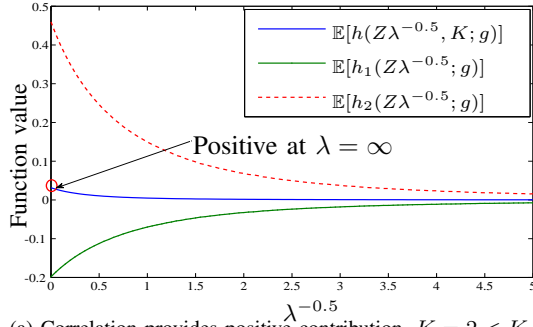
For a fixed $g(0) = M < 1$, the threshold $K_t(M)$ is

$$K_t(M) = -\frac{1}{\log(1 - M^2)} \frac{2M^2}{1 - M^2}, \tag{43}$$

and $2 < K_t(M) < \frac{2}{1 - M^2}$.

(a) Different values of correlation coefficient a, limiting correlation $M = 0.5$.

(b) Different values of limiting correlation M, correlation coefficient $a = 0.5$.

Fig. 6. Error exponent D vs. ratio of variances K for exponential correlation function, node density $\lambda = 1$. See (31), (52).

(a) Correlation provides positive contribution. $K = 2 < K_t$.

(b) Correlation provides negative contribution. $K = 2K_t$.

Fig. 7. Behavior of functions with exponential correlation $g(R) = M \exp[-aR]$, $M = 0.5, a = 1$. Functions h_1 and h_2 are independent of K. However, K affects their scaling in h. See (29).

Proof: From (41) and $\left(1 - \frac{\pi}{2\omega}\right) > 0$. □

Hence, we obtain a somewhat surprising result that at infinite node density, the effect of correlation on error exponent is different based on the variance ratio K and is determined by a threshold K_t on K. For values of K below the threshold K_t, the presence of correlation improves the error exponent in (42a). On other hand, above the threshold K_t, the presence of correlation degrades the error exponent in (42b). Moreover, at infinite density since the inter-node distances go to zero, the correlation function is given by $g(0) = M$, and hence, the threshold K_t in (42) is only a function of M.

Although the results in Lemma 3 are valid only at infinite density, we can utilize them to compare with the other extreme scenario when the density $\lambda \to 0$. In this case, the error exponent $D_\lambda \to D_{IID}$, i.e., the conditionally i.i.d. case. From Lemma 3, we can conclude that below the threshold K_t, it is better to cluster the nodes close to one another ($\lambda \to \infty$) rather than place them as far as possible ($\lambda \to 0$). On the other hand, above the threshold, the opposite is true. Hence, the results for infinite node density in Lemma 3 provide guidelines on the effect of correlation on the error exponent. In the next section, we will generalize these results to prove that the optimal node density displays a threshold behavior.

C. Threshold Behavior of Optimal Density

In this section, we provide the results for optimal density. From (36), we can rewrite density optimization in (1) as

$$\lambda_* = \arg\max_{\lambda \geq \lambda_{\bar{E}}} D_\lambda = \arg\max_{\lambda \geq \lambda_{\bar{E}}} \mathbb{E}_\lambda \, h\big(Z\lambda^{-0.5}, K; g\big), \quad (44)$$

where for the last equality, we use the fact that $D_{IID}(K)$ is independent of λ in (33).

To analyze the behavior of the expectation term in (44), we first focus on the function f in (27) given by

$$f(x, K) = \log(1 - x^2) + \frac{2}{K}\frac{x^2}{1 - x^2}, \quad \forall x \in [0, M]. \quad (45)$$

Since $g(0) = M$ and $g(\infty) = 0$, we have $x \in [0, M]$. In the lemma below, we provide results on the behavior of f.

Lemma 4 (Behavior of f): The function $f(x, K)$ in (45) with $M < 1$ satisfies

$$\arg\max_{x \in [0, M]} f(x, K) = \begin{cases} M, & K < K_t, \quad (46a) \\ 0, & \text{o.w.} \quad (46b) \end{cases}$$

Proof: See Appendix A. □

Hence, the function $f(x, K)$ attains its maximum only at one of the boundary points for $x \in [0, M]$. The particular boundary point is determined by a threshold K_t on K, as seen in (46) and also K_t depends only on M, the limiting correlation.

When the point sets are drawn from binomial or Poisson processes, and R_e are the edge-lengths of NNG , consider the

edge functional

$$\frac{1}{n} \sum_{e \in \text{NNG}} f(g(R_e), K; g).$$

From (31) and (32), we have

$$\lim_{n \to \infty} \frac{1}{n} \sum_{e \in \mathcal{E}_d} f(g(R_e), K; g) = \mathbb{E}[h(Z\lambda^{-0.5}, K; g)]. \quad (47)$$

Hence, we can use the result on the maximum of function f in Lemma 4 to find the corresponding optimal density maximizing the expectation term in (44). In the theorem below, we provide such a result on the optimal density and show that its behavior is determined only by the thresholds K_t and K_t' on K.

Theorem 4 (Result on $\lambda_*(K, \bar{E})$): The optimal density in (44) that maximizes the error exponent, under feasible average energy constraint $\bar{E}$, is given by

$$\lambda_*(K, \bar{E}) = \infty, \quad \forall K < K_t(M), \quad (48)$$

where the threshold K_t is given by (43), and

$$\lambda_*(K, \bar{E}) = \lambda_{\bar{E}} < \infty, \quad \forall K > K_t'(M), \quad (49)$$

where $\lambda_{\bar{E}}$ is defined in (36), and satisfies bounds in (40), and

$$K_t'(M) = \frac{2}{1 - M^2} > K_t(M), \quad (50)$$

where $M = g(0) < 1$ is the correlation function as the inter-node distance goes to zero. Also, when the energy constraint is infinite $\bar{E} \to \infty$, we have $\lambda_{\bar{E}} = 0$, and the result in (49) is improved to

$$\lambda_*(K, \infty) = 0, \quad \forall K > K_t(M). \quad (51)$$

Proof: See Appendix B. $\qquad\square$

The above theorem states that when the variance ratio K is below the threshold K_t, for any feasible energy constraint $\bar{E}$, optimality is attained at infinite density. On the other hand, above another threshold $K_t' > K_t$, the minimum feasible node density $\lambda_{\bar{E}}$ which supports data fusion under constraint $\bar{E}$ attains the optimal value.

In the special case, when there is infinite energy ($\bar{E} \to \infty$), we have $\lambda_1(\bar{E}) = \lambda_2(\bar{E}) = \lambda_{\bar{E}} = 0$. In this case, we prove that optimal value is zero even in the gap region between the two thresholds K_t and K_t'. Numerical investigation suggests that under any finite energy constraint, the optimal density is $\lambda_{\bar{E}}$ even in the gap region between the two thresholds K_t and K_t'.

Also interestingly, the thresholds K_t and K_t' depend on correlation $g(R)$ only through the limiting value $g(0) = M$. This is because of the behavior of the function f, elucidated in Lemma 4. We also note that as $M \to 1$, the thresholds $K_t, K_t' \to \infty$. Hence, when we approach full correlation as the inter-node distance goes to zero, the optimal node density tends towards infinity for all values of K.

D. Numerical Analysis

In this section, we plot the error exponent and optimal node density for a specific correlation function namely the exponential-correlation function,

$$g(R) = Me^{-aR}, \ a > 0, 0 < M < 1. \quad (52)$$

Using Theorem 3, we numerically evaluate D through Monte-Carlo runs. In (31), the error exponent is an implicit function of the correlation coefficient a, through the correlation function g. We plot the effects of correlation coefficient a and limiting correlation M on D in Fig.6.

In Fig.6(a), we plot the error exponent at $\lambda = 1$ and $M = 0.5$, for different values of correlation coefficient a. We notice that a more correlated GMRF or the one with smaller a, has a higher exponent at low value of K, whereas the situation is reversed at high K. Also, when the variance ratio K is large enough, D appears to increase linearly with K (in dB), and the correlation coefficient a and the limiting correlation M appear to have little effect, as expected from Theorem 3. In Fig.6(b), we plot the exponent at constant correlation coefficient $a = 0.5$ for different values of the limiting correlation M. Also note, $M = 0$ reduces to the independent case. We notice a similar behavior as the correlation coefficient a in Fig.6(a). A higher value of M results in a higher exponent at low K, but not at high K.

In Fig.7, we fix the correlation coefficient $a = 1$ in (52), and plot the expectations of functions h, h_1 and h_2 against $\lambda^{-0.5}$. In Fig.7a and Fig.7b, the value of K is below and above the threshold K_t. We observe that the behavior at $\lambda = \infty$ is different in the two plots. Note that the functions h_1 and h_2 are independent of K, but K affects their scaling in h.

In Fig.8a and Fig.8b, we numerically evaluate the optimal $\lambda_*(K, \lambda_{\bar{E}})$ for different values of M and variance ratio K. It is convenient to plot the results in terms of $\lambda^{-0.5}$, since the optimal λ_* is infinite when K is below the threshold K_t. We observe the threshold behavior at K_t, as predicted in Theorem 4: when $K < K_t$, we have $\lambda_* = \infty$ and for $K > K_t$, in Fig.8a and Fig.8b, optimality is mostly attained at the other extreme point $\lambda_{\bar{E}}$. This is consistent with Theorem 4.

E. Sensitivity Analysis

In Theorem 4, we proved the result on the optimal density λ_*. In this section, we analyze the extent to which the error exponent is dependent on λ. This enables us to gauge the usefulness of finding λ_*. To this end, we define

$$\Gamma(\lambda, K; g) := \frac{\mathbb{E}[Z\lambda^{-0.5}, K; g]}{2D(\lambda, K; g)}, \quad (53)$$

which is the fraction of contribution coming from correlation to the error exponent in (33), and hence, it is the part influenced by λ. Note, $0 \le \Gamma(\lambda, K; g) \le 1$ and $\Gamma(0, K; g) = 0$.

Lemma 5 (Sensitivity of D_λ to λ): At $K = 1$, the fraction of contribution from correlation to the error exponent $\Gamma(\lambda, K; g)$ is maximum,

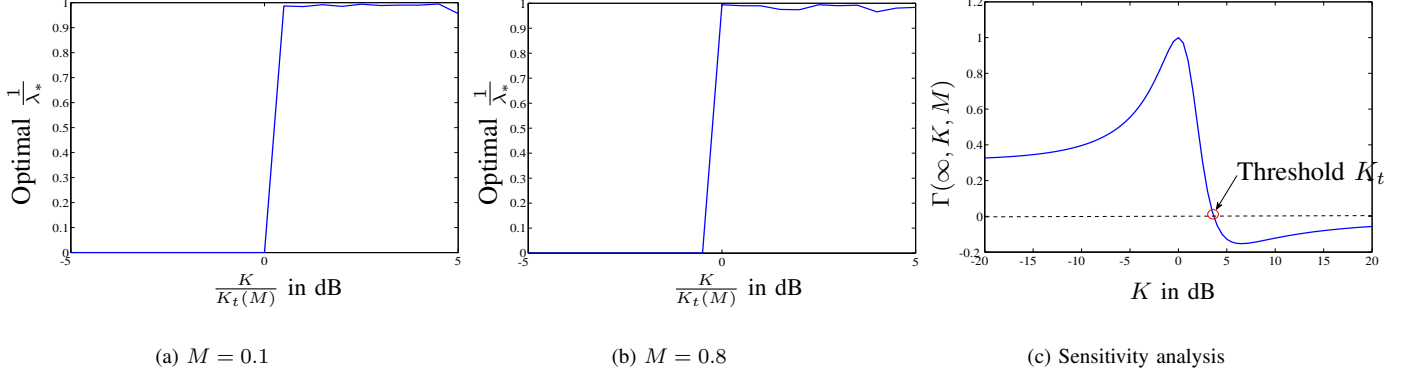(a) $M = 0.1$ (b) $M = 0.8$ (c) Sensitivity analysis

Fig. 8. [a,b] The optimal density λ_* is decided by threshold $K_t(M)$ on variance ratio K. $\lambda_{\bar{E}} = 1$. See Theorem 4. [c] The contribution from correlation to error exponent vs. variance ratio K at $\lambda = \infty$ and $M = 0.5$. See (53).

$$\Gamma(\lambda, 1; g) = 1, \quad \forall \lambda > 0. \tag{54}$$

Also, in the large-K regime,

$$\Gamma(\lambda, K; g) \to 0, \quad \text{as } K \to \infty, \forall \lambda \in \Re^+. \tag{55}$$

Hence, node density greatly influences detection performance at $K = 1$. Intuitively, this is because at $K = 1$, the two hypotheses can only be distinguished through the presence of correlation under $\mathcal{H}_1$. We also see that it decays to zero as $K \to \infty$. Hence, the error exponent is insensitive to changes in density at high K. In Fig.8c, we plot $\Gamma(\lambda, K; g)$ as a function of K.

IX. ENERGY-DENSITY CONSTRAINT

We now analyze the optimal node density under a different formulation. Instead of having fixed number of nodes placed in varying areas under a given constant node density, in this section, we fix areas of deployment A according to a constant node density λ and then, let $A \to \infty$. This means that we now have the flexibility of placing few powerful nodes or many cheaper nodes in a given area. On the other hand, earlier we had the option of choosing the area of deployment for a fixed number of nodes.

Under this formulation, the processing energy C_p at each node needs to be incorporated. We impose an energy density constraint κ

$$\kappa \geq \lim_{C,A\to\infty} \frac{C}{A}, \tag{56}$$

where C is the total (routing + processing) energy consumption C in area A. Hence, we impose a constraint on the energy consumption per unit area, instead of a constraint on the average energy consumption per node, as in (1).

The error exponent D_λ^p with respect to total energy C is

$$D_\lambda^p := \lim_{C\to\infty} -\frac{1}{C} \log P_M(C). \tag{57}$$

The optimal density λ_*^p under the energy-density constraint is

$$\lambda_*^p := \max_{\lambda \in \Re^+} D_\lambda^p, \tag{58}$$

subject to the energy-density constraint κ in (56).

Note that the error exponent D_λ^p with respect to the total energy C can be expressed as

$$D_\lambda^p = \frac{D_\lambda}{\bar{C}(\lambda)}, \tag{59}$$

where D_λ is the error exponent with respect to number of nodes and $\bar{C}(\lambda)$ is the average energy per node, dealt in the previous sections. Similarly, the energy density constraint simplifies to

$$\kappa \geq \lim_{C,A\to\infty} \frac{C}{A} \approx \lambda \frac{C}{\lfloor \lambda A \rfloor} = \lambda \bar{C}(\lambda), \quad \lambda \in \Re^+, \tag{60}$$

since $\lfloor \lambda A \rfloor$ is the number of nodes and the approximation consists of ignoring the integer requirement for the number of nodes. We again define Λ for this setup to be the set of the feasible node densities under minimum energy routing

$$\Lambda := \{\lambda : \lambda \bar{C}_*(\lambda) \leq \kappa\}. \tag{61}$$

In the theorem below, we show the finiteness of λ_p^*. We note that this result is on lines of the results in [25] for a one dimensional GMRP.

Theorem 5 (Finite λ_*^p): The optimal density λ_*^p in (58) exists whenever the set Λ in (61) is non-empty and λ_*^p is additionally finite if the per-node processing energy $C_p > 0$.

Proof: Note that a compact set possesses a finite extremum point. To show that Λ is a compact set, we first note that Λ is a closed set. To show the bounded property, note that

$$\lambda \bar{C}(\lambda) \sim \lambda [C_p + c\lambda^{-\frac{\nu}{2}}] \to \infty, \quad \text{as } \lambda \to \infty.$$

Hence, the constraint κ in (60) is violated as $\lambda \to \infty$ and hence, ∞ cannot be in Λ. Hence, Λ is closed and bounded, i.e., compact. This implies that $\lambda_*^p \in \Lambda$ is finite. $\square$

In the above theorem, note that for the feasible set Λ to be non-empty, the constraint κ has to be sufficiently large.
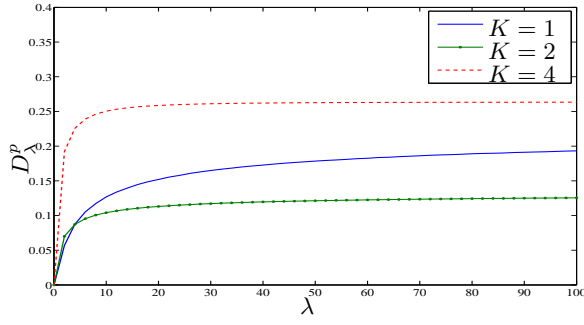
Fig. 9. The error exponent D_λ^p with respect to the total energy. See (57). $\nu = 2, C_p = 1, C_t = \frac{1}{c_1(2)}, M = 0.6$.

In other words, we need a large enough energy density κ to support energy consumption involved in processing and routing of measurements.

We observe that there is no threshold effect when there is a energy-density constraint and the optimal node density λ_*^p is always finite. This is in sharp contrast with the results in the previous section, where under the per-node energy constraint, λ_* can be unbounded depending on the regime of K. This is because here, the energy-density constraint κ limits the energy consumption in a given area thereby making infinite density infeasible. This implies that λ_*^p cannot be unbounded. In the theorem below, we provide bounds for λ_*^p when the variance ratio $K < 2$, based on the monotonicity of the error exponent in this regime.

Theorem 6 (Optimal λ_*^p): Let $\lambda_i^p(\kappa)$ be the largest (positive real) root of the equation,

$$\lambda C_p + \lambda^{1-\frac{\nu}{2}} C_t c_i(\nu) - \kappa = 0, \quad \text{for } i = 1, 2. \quad (62)$$

where $c_1(\nu)$ and $c_2(\nu)$ are the energy-scaling constants in (24). If the per-node processing energy $C_p > 0$, the variance ratio $K < 2$ and the constraint κ is such that both $\lambda_1^p(\kappa)$ and $\lambda_2^p(\kappa)$ exist then the optimal λ_*^p satisfies

$$\lambda_2^p(\kappa) \leq \lambda_*^p \leq \lambda_1^p(\kappa). \quad (63)$$

Proof: On the lines of the arguments in the previous section, it can be shown that D_λ is increasing in λ for $K < 2$. From (24), $\bar{C}_*(\lambda)$ is decreasing in λ. Hence, the exponent D_λ^p in (57) is increasing in λ. From the energy-density constraint in (60) and Theorem 5, the feasible set Λ is bounded. From the bounds on $\bar{C}_*(\lambda)$ in (24), if the largest real roots of (62), for $i = 1, 2$, exist, then the maximum value in Λ is bounded by these roots. □

Hence, in the above theorem, we obtain bounds on the optimal density λ_*^p under energy-density formulation. We prove this by first showing that the error exponent D_λ^p is increasing with λ when the variance ratio $K < 2$, as seen in Fig. 9. This implies that λ_*^p is the largest feasible density under constraint κ that supports the energy consumption for data fusion. In the end, we provide the bounds in (63) on this largest feasible density through the bounds for average energy consumption $\bar{C}_\lambda$ in (24). Although we analytically prove the

bounds in (63) only when the variance ratio $K < 2$, the behavior of the error exponent D_λ^p in Fig.9 suggests that the bound in (63) may be valid for all values of K.

X. CONCLUSIONS

The tradeoff between the energy consumption in data fusion and the resulting detection performance at the fusion center is an important problem in the context of sensor networks. In this paper, we incorporated correlation between the measurements through the Gauss-Markov random field model. We characterized the density of node deployment that maximizes the detection error exponent subject to a constraint on the average energy consumption. The measurement variance is crucial in determining whether the optimal node density is limited by the fusion energy constraint and displays a threshold behavior. We derived the threshold analytically and verified it with simulations.

The results on the optimal density are possible due to exploitation of the Markovian structure, in deriving the error exponent and the fusion schemes. While acknowledging the limitations of its validity, we have made an attempt to characterize detection-energy tradeoffs for correlated measurements in two (and higher) dimensional spaces, which to the best of our knowledge, has not been dealt before.

Alternative formulations, not dealt in this paper, include selection of nodes with "useful" data [30], and incorporating node and link failures. We have also not considered the issue of quantization of measurements, a difficult problem even for conditionally i.i.d. measurements and the recent works in [40], [41] have considered it for tree and tandem network topologies. Another issue not addressed is that of the latency involved for the decision to be made at the fusion center. Extension of this work to incorporate more general dependencies among sensor measurements is currently under investigation.

APPENDIX

A. Proof of Lemma 4

Since $g(0) = M$ and $g(\infty) = 0$, we have $x \in [0, M]$.

$$\frac{\partial f}{\partial x} = \frac{2x}{1 - x^2}\left(-1 + \frac{2}{K(1 - x^2)}\right).$$

Therefore, f has only one critical point in $(0, M)$. For $K < 2$, $\frac{\partial f}{\partial x} > 0$ and for $K > K_t'$, $\frac{\partial f}{\partial x} < 0$, $\forall x \in [0, M]$. There are no critical points. For $2 < K < K_t'$, the critical point is a minimum. Hence, maximum is attained at one of the boundary points $\{0, M\}$. For $K < K_t$, it is at $x = M = g(0)$ and hence,

$$f(g(R_e), K) \leq f(g(0), K; g), \quad \forall R_e \geq 0.$$

Similarly, for $K > K_t$, we have

$$f(R_e, K; g) \leq f(\infty, K; g) = 0, \quad \forall R_e \geq 0.$$

B. Proof of Theorem 4

From Lemma 4, when $K < K_t$, $g(0) = M$ attains the maximum of $f(g(R_e), K)$. Hence, we have for $R_e \geq 0$,

$$\frac{1}{n} \sum_{e \in \mathcal{E}_d} f(g(R_e), K; g) \leq \frac{1}{n} \sum_{e \in \mathcal{E}_d} f(g(0), K; g), \quad \forall K < K_t.$$

Letting $n \to \infty$ on both sides, from (47)

$$\mathbb{E}[h(Z\lambda^{-0.5}, K; g)] \leq h(0, K, M), \quad \forall K < K_t.$$

Hence, the optimal density in this regime is given by

$$\lambda_*(K, \bar{E}) = \arg \max_{\lambda \geq \lambda_{\bar{E}}} \mathbb{E}[h(Z\lambda^{-0.5}, K; g)] = \infty \quad \forall K < K_t.$$

From Lemma 4, when $K > K_t$, $g(\infty) = 0$ attains the maximum of $f(g(R_e), K)$. For the case of infinite energy $\bar{E} \to \infty$, $\lambda_{\bar{E}} = \lambda_2(\bar{E}) = \lambda_1(\bar{E}) = 0$. Hence,

$$\lambda_*(K, \infty) = \arg \max_{\lambda \geq \lambda_{\bar{E}}=0} \mathbb{E}[h(Z\lambda^{-0.5}, K; g)] = 0 \quad \forall K > K_t.$$

For finite constraint $\bar{E}$ and $K > K_t'$, $f(g(R_e), K)$ is increasing in R_e. We have $R_e = \lambda^{-0.5} R_e'$, where R_e' is the edge-length in unit area and is independent of λ. Hence, $f(g(R_e), K)$ is non-increasing in λ and the limit $\mathbb{E}[h(Z\lambda^{-0.5}, K; g)]$ is also non-increasing in λ. Hence,

$$\lambda_*(K, \bar{E}) = \arg \max_{\lambda \geq \lambda_{\bar{E}}} \mathbb{E}[h(Z\lambda^{-0.5}, K; g)] = \lambda_{\bar{E}} \quad \forall K > K_t'.$$

$\square$

REFERENCES

[1] A. Anandkumar, L. Tong, and A. Swami, "Detection of Gauss-Markov Random Fields under Routing Energy Constraint," in *Proc. of 45-th Allerton Conf. on Communication, Control and Computing*, Monticello, USA, Sept. 2007.

[2] ——, "Detection of Gauss-Markov random fields with nearest-neighbor dependency," *Submitted to IEEE Trans. Information Theory*, Dec. 2006, available on Arxiv.

[3] ——, "Energy Efficient Routing for Statistical Inference of Markov Random Fields," in *Proc. of CISS '07*, Baltimore, USA, March 2007, pp. 643–648.

[4] A. Deshpande, C. Guestrin, S. Madden, J. Hellerstein, and W. Hong, "Model-driven data acquisition in sensor networks," in *VLDB*, 2004.

[5] R. Cristescu and M. Vetterli, "On the optimal density for real-time data gathering of spatio-temporal processes in sensor networks," in *IPSN*, 2005, pp. 159–164.

[6] D. Marco, E. Duarte-Melo, M. Liu, and D. Neuhoff, "On the many-to-one transport capacity of a dense wireless sensor network and the compressibility of its data," in *Proc. IPSN*, 2003, pp. 1–16.

[7] S. Yoon and C. Shahabi, "The Clustered Aggregation technique leveraging spatial and temporal correlations in wireless sensor networks," *ACM Transactions on Sensor Networks*, vol. 3, no. 1, 2007.

[8] J. Faruque and A. Helmy, "RUGGED: RoUting on finGerprint Gradients in sEnsor Networks," in *IEEE/ACS Intl. Conf. on Pervasive Services (ICPS)*, 2004, pp. 179–188.

[9] S. Pattem, B. Krishnamachari, and R. Govindan, "The impact of spatial correlation on routing with compression in wireless sensor networks," in *Proceedings of the third international symposium on Information processing in sensor networks*, 2004, pp. 28–35.

[10] J. Besag, "Spatial interaction and the statistical analysis of lattice systems," *Journal of Royal Stat. Soc.*, vol. 36, no. B, pp. 192–225, 1974.

[11] ——, "Statistical analysis of non-lattice data," *The Statistician*, vol. 24, no. 3, pp. 179–195, 1975.

[12] M. Cetin, L. Chen, J. Fisher, A. Ihler, O. Kreidl, R. Moses, M. Wainwright, J. Williams, and A. Willsky, "Graphical Models and Fusion in Sensor Networks," in *Wireless sensor networks: signal processing & comm. perspectives*. J. Wiley & Sons, 2007, ch. 9, pp. 215–250.

[13] S. Li, *Markov random field modeling in computer vision*. Springer-Verlag London, 1995.

[14] N. Cressie, *Statistics for spatial data*. J. Wiley, 1993.

[15] T. Kailath and H. Poor, "Detection of stochastic processes ," *IEEE Trans. on Information Theory*, vol. 44, no. 6, pp. 2230–2259, Oct. 1998.

[16] M. D. Donsker and S. R. S. Varadhan, "Large deviations for stationary Gaussian process," *Commun. Math. Phys.*, vol. 97, pp. 187–210, 1985.

[17] P.-N. Chen, "General formulas for the Neyman-Pearson type-II error exponent subject to fixed and exponential type-I error bounds," *IEEE Trans. on Information Theory*, vol. 42, no. 1, pp. 316–323, Jan. 1996.

[18] A. Giridhar and P. Kumar, "Toward a theory of in-network computation in wireless sensor networks," *Comm. Magazine, IEEE*, vol. 44, no. 4, pp. 98–107, 2006.

[19] R. Rajagopalan and P. Varshney, "Data aggregation techniques in sensor networks: A survey," *Comm. Surveys & Tutorials, IEEE*, vol. 8, no. 4, pp. 48–63, 2006.

[20] K. Akkaya and M. Younis, "A Survey of Routing Protocols in Wireless Sensor Networks," *Elsevier Adhoc Networks*, vol. 3, pp. 325–349, 2005.

[21] Y. Yang and R. Blum, "Energy-efficient routing for signal detection under the Neyman-Pearson criterion in wireless sensor networks," in *Proc. IPSN*, 2007, pp. 303–312.

[22] S. Appadwedula, V. Veeravalli, and D. Jones, "Energy-Efficient Detection in Sensor Networks," *IEEE J. Select. Area Comm.*, vol. 23, no. 4, pp. 693–702, 2005.

[23] L. Yu, L. Yuan, G. Qu, and A. Ephremides, "Energy-driven detection scheme with guaranteed accuracy," in *Proc. IPSN*, 2006, pp. 284–291.

[24] Y. Sung, S. Misra, L. Tong, and A. Emphremides, "Cooperative Routing for Signal Detection in Large Sensor Networks," *IEEE J. Select. Area Comm.*, vol. 25, no. 2, pp. 471–483, 2007.

[25] J. Chamberland and V. Veeravalli, "How Dense Should a Sensor Network Be for Detection With Correlated Observations?" *Information Theory, IEEE Transactions on*, vol. 52, no. 11, pp. 5099–5106, 2006.

[26] N. Katenka, E. Levina, and G. Michailidis, "Local vote decision fusion for target detection in wireless sensor networks," in *Joint Research Conf. on Statistics in Quality Industry and Tech.*, Knoxville, USA, June 2006.

[27] O. Kreidl and A. Willsky, "Inference with Minimal Communication: a Decision-Theoretic Variational Approach," in *Advances in Neural Information Processing Systems*, 2006.

[28] A. Anandkumar, L. Tong, A. Swami, and A. Ephremides, "Minimum Cost Data Aggregation with Localized Processing for Statistical Inference," in *Proc. of IEEE INFOCOM*, Phoenix, USA, April 2008, pp. 780–788.

[29] A. Anandkumar, A. Ephremides, L. Tong, and A. Swami, "Minimum cost routing with local processing for distributed statistical inference," in *Handbook on Array Processing and Sensor Networks*, S. Haykin and R. Liu, Eds. IEEE-Wiley, 2008, ch. 25.

[30] A. Anandkumar, L. Tong, A. Swami, and A. Ephremides, "Cost-Performance Tradeoff in Multi-hop Aggregation for Statistical Inference," in *Proc. of IEEE International Symposium on Information Theory*, Toronto, Canada, July 2008.

[31] M. Penrose and J. Yukich, "Limit Theory for Random Sequential Packing and Deposition," *Annals of Applied probability*, vol. 12, no. 1, pp. 272–301, 2002.

[32] H. Rue and L. Held, *Gaussian Markov Random Fields: Theory and Applications*. London: Chapman and Hall, 2005.

[33] A. Ephremides, "Energy concerns in wireless networks," *IEEE Wireless Communications*, no. 4, pp. 48–59, August 2002.

[34] M. Penrose and J. Yukich, "Central limit theorems for some graphs in computational geometry," *Annals of Applied probability*, vol. 11, no. 4, pp. 1005–1041, 2001.

[35] J. Moura and N. Balram, "Recursive Structure of Noncausal Gauss-Markov Random Fields," *IEEE Trans. IT*, vol. IT-38, no. 2, pp. 334–354, March 1992.

[36] J. Møller and R. Waagepetersen, *Statistical Inference and Simulation for Spatial Point Processes*. Chapman & Hall/CRC, 2004.

[37] J. Steele, *Probability theory and combinatorial optimization*. Society for Industrial and Applied Mathematics Philadelphia, 1997.

[38] M. Penrose and J. Yukich, "Weak laws of large numbers in geometric probability," *Annals of Applied probability*, vol. 13, no. 1, pp. 277–303, 2003.

[39] M. Cortina-Borja and T. Robinson, "Estimating the asymptotic constants of the total length of Euclidean minimal spanning trees with power-

weighted edges," *Statistics and Probability Letters*, vol. 47, no. 2, pp. 125–128, 2000.

[40] W. P. Tay, J. N. Tsitsiklis, and M. Z. Win, "Data fusion trees for detection: Does architecture matter?" *IEEE Tran. on Information Theory*, 2007, submitted for publication.

[41] ——, "On the sub-exponential decay of detection error probabilities in long tandems," *IEEE Tran. on Information Theory*, 2007, submitted for publication.

Animashree Anandkumar (S '02) received the B.Tech degree in Electrical Engineering from Indian Institute of Technology Madras, Chennai, India in 2004. She is currently pursuing her Ph.D. degree in Electrical Engineering at Cornell University, Ithaca, NY. She has been a member of the Adaptive Communications and Signal Processing Group (ACSP) at Cornell University since August, 2004.

Anima received the Fran Allen IBM Ph.D fellowship for the year 2008-09, presented annually to one female Ph.D. student in conjunction with the IBM Ph.D. Fellowship Award, in recognition of her technical accomplishments, as well as her commitment to mentoring and community building. She was named a finalist for the Google Anita-Borg Scholarship 2007-08. She received the Student Paper Award at the 2006 International Conference on Acoustic, Speech and Signal Processing (ICASSP) held at Toulouse, France.

Anima Anandkumar's research interests are in the area of statistical-signal processing, information theory and networking. Specifically, she has been working on detection and estimation, asymptotic analysis and in-network function computation, in the context of wireless-sensor networks. She has served as a reviewer for IEEE transactions on signal processing, IEEE transactions on information theory and various IEEE conferences.
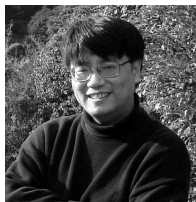
Lang Tong (S'87,M'91,SM'01,F'05) is the Irwin and Joan Jacobs Professor in Engineering at Cornell University Ithaca, New York. Prior to joining Cornell University, he was on faculty at the West Virginia University and the University of Connecticut. He was also the 2001 Cor Wit Visiting Professor at the Delft University of Technology. Lang Tong received the B.E. degree from Tsinghua University, Beijing, China, in 1985, and M.S. and Ph.D. degrees in electrical engineering in 1987 and 1991, respectively, from the University of Notre Dame, Notre Dame, Indiana. He was a Postdoctoral Research Affiliate at the Information Systems Laboratory, Stanford University in 1991.

Lang Tong is a Fellow of IEEE. He received the 1993 Outstanding Young Author Award from the IEEE Circuits and Systems Society, the 2004 best paper award (with Min Dong) from IEEE Signal Processing Society, and the 2004 Leonard G. Abraham Prize Paper Award from the IEEE Communications Society (with Parvathinathan Venkitasubramaniam and Srihari Adireddy). He is also a coauthor of five student paper awards. He received Young Investigator Award from the Office of Naval Research.

Lang Tong's research is in the general area of statistical signal processing, wireless communications and networking, and information theory. He has served as an Associate Editor for the IEEE Transactions on Signal Processing, the IEEE Transactions on Information Theory, and IEEE Signal Processing Letters.

Ananthram Swami received the B.Tech. degree from IIT-Bombay; the M.S. degree from Rice University, and the Ph.D. degree from the University of Southern California (USC), all in Electrical Engineering. He has held positions with Unocal Corporation, USC, CS-3 and Malgudi Systems. He was a Statistical Consultant to the California Lottery, developed a Matlab-based toolbox for non-Gaussian signal processing, and has held visiting faculty positions at INP, Toulouse. He is currently with the US Army Research Laboratory where his work is in the broad area of signal processing, wireless communications, sensor and mobile ad hoc networks.

He has served as associate editor of the IEEE Transactions on Wireless Communications, IEEE Signal Processing Letters, IEEE Transactions on Circuits & Systems-II, IEEE Signal Processing Magazine, and IEEE Transactions on Signal Processing. He was co-guest editor of a 2004 Special Issue (SI) of the IEEE Signal Processing Magazine (SPM) on 'Signal Processing for Networking', a 2006 SPM SI on 'Distributed signal processing in sensor networks', a 2006 EURASIP JASP SI on Reliable Communications over Rapidly Time-Varying Channels', a 2007 EURASIP JWCN SI on 'Wireless mobile ad hoc networks', and is the Lead Editor for a 2008 IEEE JSTSP SI on "Signal Processing and Networking for Dynamic Spectrum Access". He is a co-editor, with Qing Zhao, Yao-Win Hong and Lang Tong, of the 2007 Wiley book "Wireless Sensor Networks: Signal Processing & Communications Perspectives".